Journal of Quantitative Spectroscopy & Radiative Transfer 153 (2015) 65–76

Contents lists available at ScienceDirect

Journal of Quantitative Spectroscopy & Radiative Transfer

journal homepage: www.elsevier.com/locate/jqsrt

Comparison of CERES-MODIS cloud microphysical properties with surface observations over Loess Plateau

Hongru Yan [a], Jianping Huang [a,*], Patrick Minnis [b], Yuhong Yi [e], Sunny Sun-Mack [c], Tianhe Wang [a], Takashi Y. Nakajima [d]

[a] Key Laboratory for Semi-Arid Climate Change of the Ministry of Education, College of Atmospheric Sciences, Lanzhou University, Lanzhou 730000, China
[b] NASA Langley Research Center, Hampton, VA 23666, USA
[c] Science Systems and Applications Incorporated, Hampton, VA 23666, USA
[d] Research and Information Center, Tokai University, Tokyo, Japan
[e] Key Laboratory of Western China's Environmental Systems, Ministry of Education, Research School of Arid Environment and Climate Change, Lanzhou University, Lanzhou 730000, China

ARTICLE INFO

Article history:
Received 8 May 2014
Received in revised form
6 September 2014
Accepted 8 September 2014
Available online 18 September 2014

Keywords:
Validation
Cloud microphysical properties
Satellite

ABSTRACT

To enhance the utility of satellite-derived cloud properties for studying the role of clouds in climate change and the hydrological cycle in semi-arid areas, it is necessary to know their uncertainties. This paper estimates the uncertainties of several cloud properties by comparing those derived over the China Loess Plateau from the MODerate-resolution Imaging Spectroradiometer (MODIS) on Terra and Aqua by the Clouds and Earth's Radiant Energy System (CERES) with surface observations at the Semi-Arid Climate and Environment Observatory of Lanzhou University (SACOL). The comparisons use data from January 2008 to June 2010 limited to single layer and overcast stratus conditions during daytime. Cloud optical depths (τ) and liquid water paths (LWP) from both Terra and Aqua generally track the variation of the surface counterparts with modest correlation, while cloud effective radius (r_e) is only weakly correlated with the surface retrievals. The mean differences between Terra and the SACOL retrievals are -4.7 ± 12.9, 2.1 ± 3.2 μm and 30.2 ± 85.3 g m^{-2} for τ, r_e and LWP, respectively. The corresponding differences for Aqua are 2.1 ± 8.4, 1.2 ± 2.9 μm and 47.4 ± 79.6 g m^{-2}, respectively. Possible causes for biases of satellite retrievals are discussed through statistical analysis and case studies. Generally, the CERES-MODIS cloud properties have a bit larger biases over the Loess Plateau than those in previous studies over other locations.

1. Introduction

Clouds, covering about 60% of the Earth's surface, are responsible for up to two-thirds of the planetary albedo, which is about 30%. Clouds not only play an important role in the energy budget of Earth-atmospheric system, but are also critical in the hydrological cycle. Simultaneously, clouds remain a major source of uncertainty in the simulation of climate changes due to its complex feedback [4–6,3,16,28,43,45,51,41,14]. Cloud amount, height, optical thickness, liquid water path and droplet effective radius are generally used as simplified representations of cloud physics in recent generations of models. Using adequate data to constrain models is necessary to solve this problem. And the critical prerequisite of that is to increase the knowledge of accuracy and stability of global climatic datasets from space.

The National Aeronautics and Space Administration (NASA) CERES project [54] was created to investigate the

* Corresponding author. Tel.: +86 931 8914282.
E-mail address: hjp@lzu.edu.cn (J. Huang).

http://dx.doi.org/10.1016/j.jqsrt.2014.09.009
0022-4073/

Table 1
Surface-derived cloud properties and their uncertainties.

Cloud properties	Uncertainty	Instrument/retrieval algorithm
Cloud optical depth	$<5\%$	[31,49]
Cloud liquid water path	~ 20 g m^{-2} (LWP <250 g m^{-2})	[25]
	~ 32 g m^{-2} (LWP >250 g m^{-2})	[22]
Cloud droplet effective radius	~ 1.5 μm (LWP <250 g m^{-2})	[30]
	~ 3 μm (LWP >250 g m^{-2})	

critical role that clouds play in modulating the radiative energy flow within the Earth-atmosphere system by providing long-term highly accurate solar-reflected and Earth-emitted radiation from the top of the atmosphere to the Earth's surface, and coincident cloud and aerosol properties inferred from high-resolution imager measurements such as the MODerate-resolution Imaging Spectroradiometer (MODIS) on the Terra and Aqua satellites [52,53]. The long-term CERES cloud and radiative flux data are helping to improve our understanding of the relationships between clouds and the radiation budget and are valuable for the advancement of climate models (e.g., [48]). So it is urgent to estimate the uncertainties of cloud properties in the CERES datasets by comparing them with well-validated surface retrievals of the same parameters.

Validations of the CERES cloud property retrieval system (CPRS) algorithms have been performed over a variety of sites in various climate regimes. Dong et al. [11] compared the retrievals of liquid cloud droplet size and optical depth derived using the CPRS and found good agreement with the surface and in situ data over the Arctic ice pack. CPRS-derived cirrus cloud properties were compared with radar [27] and radiometer [32] retrievals over the Southern Great Plains (SGP) site in Oklahoma. Other comparisons with data taken at the SGP and other locations have been performed (e.g., [44,46,12,13,36,57]), but not yet over the interior of Asia or any other arid regions, where severe shortages of water resources are common and dust storms frequently originate. Because clouds are a potential sustainable water resource for arid and semi-arid regions, small changes in cloud amount, altitude, physical thickness, and/or microphysical properties can alter the surface radiation budget and hydrological cycle over such areas. As Fu et al. [15] indicated, semi-arid lands, especially those located in mid-latitude inner continental regions, are some of the most sensitive areas to climate change. Nevertheless, scarce ground-based observations limit validation of satellite retrievals over those areas. The Semi-Arid Climate and Environment Observatory of Lanzhou University (SACOL, 35°57′N, 104°08′E, Elev. 1965.8 m) located in the Northwest of China, which is the only international long-term climate observatory over the Loess Plateau of China, was established in 2005 and its data can fill one of the major gaps in the surface network of observations needed to validate space-borne cloud retrievals [21].

To begin the process of validating satellite-based cloud properties over central Asia, this paper presents a comparison of daytime-only stratus overcast cloud properties derived from CERES-MODIS data with ground-based retrievals from January 2008 to June 2010 at SACOL. An exhaustive validation of all cloud properties is a complex and challenging process. Thus, for simplicity, emphasis is placed solely on assessing CERES-derived MODIS properties of single-layer, overcast water clouds over this site. A brief description of surface and satellite retrievals is presented in Section 2. Statistical comparisons of the surface and satellite-derived cloud properties are presented in Section 3 along with several case studies. Section 4 presents the summary and conclusions.

2. Data and methods

2.1. Surface data

Ground-based retrievals of cloud microphysical properties are derived from measurements at the SACOL, which is located on the China Loess Plateau, where is a typical semi-arid region and the surface is mainly covered by short grass, which is usually less than 15-cm tall and covers around or less than 80% of the surface in summer and autumn. During spring and winter, the underlay of SACOL is short glass or barren [50]. SACOL has participated in the Coordinated Energy and water cycle Observations Project (CEOP) and is a member of the AErosol RObotic NETwork (AERONET) and the Micro-Pulse Lidar NETwork (MPLNET). The quality of data measured at SACOL is guaranteed by using precision instruments with daily maintenance and quality control. The SACOL ground-based retrievals of cloud properties, as well as their uncertainties, retrieval algorithms and period of measurement in this study are listed in Table 1. Basic information about clouds over SACOL is provided by a TP/WVP-3000 Microwave Radiometer (MWR), a Multi-Filter Rotating Shadowband Radiometer (MFRSR), a Micro-Pulse Lidar (MPL) and a Total Sky Imagery (TSI). The cloud optical depth (τ) at the SACOL is retrieved from the measurements of an unfiltered silicon pyranometer and the MFRSR, which is a seven-channel radiometer with six bands of 10-nm FWHM (full width at half maximum) centered near 415, 500, 610, 665, 862, and 940 nm. For retrieval of both liquid and ice cloud optical depth, we take advantage of simultaneous spectral measurements of direct-beam and total radiation from MFRSR and differences in the ice and liquid cloud particle scattering phase functions [30,31,49]. Compared to other surface-based retrieval techniques, this method develops a simple correction scheme that effectively removes radiation scattered in the forward direction by a cloud [23]. For the nominal possible instrument noise and uncertainties, the accuracy for cloud optical depth under homogeneous condition is 5%. And the errors in the profile of effective radius can add another 2% or 3% uncertainty to the optical

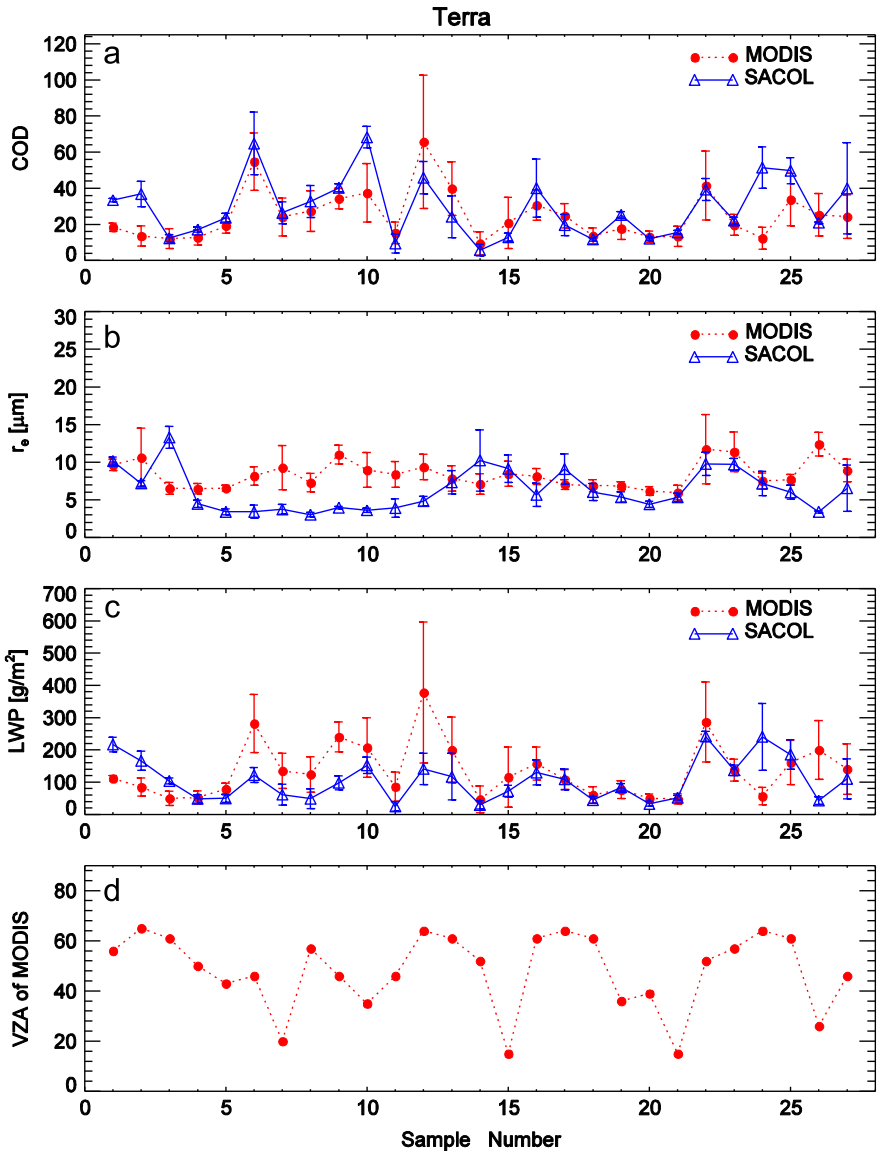

Fig. 1. Time series of surface-derived (1-h average) and matched Terra MODIS-derived cloud microphysical properties (20-km radius average), (a) cloud liquid water path, (b) cloud optical depth, (c) cloud effective radius, and (d) satellite viewing zenith angle, for daytime single layer, overcast stratus clouds over the SACOL. The error bars on the satellite and SACOL data points indicate the corresponding standard deviation of average pixels and samples.

depth. The cloud liquid water path (LWP) is retrieved from MWR measurements of brightness temperatures at 23.8 and 30 GHz using an improved statistical retrieval method [25,22], the error is about 20 g m^{-2} for LWP less than 250 g m^{-2} and about 32 g m^{-2} for greater LWP values. In addition, the cloud droplet particle size, or effective radius (r_e), is derived from the ratio of LWP and τ as stated in Min and Harrison [30] with errors of 1.5 and 3 μm for LWP less than 250 g m^{-2} and greater LWP values, respectively.

2.2. Satellite data

To avoid the uncertainty from point spread function and parallel errors, which is raised from the plane-parallel homogeneous cloud assumption, in CERES large footprint (nadir resolution 20-km equivalent diameter), pixel-level cloud properties derived from the Terra/Aqua MODIS using CERES Edition-2 algorithms are used in this study. To infer cloud properties, CERES uses a 1-km resolution MODIS Collection-5 radiance subset that has been sub-sampled to include only the data that corresponds to every fourth pixel and every second scan line.

Six cloud masks were developed to classify MODIS pixels for CERES as either cloudy or clear in nonpolar [33] and polar regions [47] during daytime (solar zenith angle, SZA $< 82^\circ$), twilight ($82^\circ \leq$ SZA $\leq 88.5^\circ$), and nighttime (SZA $> 88.5^\circ$). Each clear or cloudy pixel is further classified as "weak" or "strong" to indicate the degree of confidence in each pixel's classification. These masks use

the 0.64 (VIS), 1.62, 3.78, 10.8 (IR), and 12.0-μm channels from MODIS.

The Visible-Infrared-Shortwave-infrared-Split-window Technique (VISST) is applied to retrieve CERES-MODIS cloud microphysical parameters over snow-free areas in daytime [35]. Given the spectral clear-sky radiances and surface properties for a particular set of SZAs, viewing zenith angles VZA, and relative azimuth angles, the VISST computes the spectral radiances expected at the top of the atmosphere TOA for both water droplet and ice crystal clouds over a range of optical depths from 0.25 to 128 for a particular cloud temperature. The values of r_e for modeled clouds range from 2 to 32 μm for liquid water clouds. The modeled TOA radiances include the attenuation of the radiation by the atmosphere and the impact of the radiation emitted or reflected by the surface. VISST relies on the IR radiance to retrieve cloud effective temperature (Te), the 3.78-μm radiance to estimate effective droplet radius (r_e), the VIS reflectance to obtain cloud optical depth (τ) and the 12.0-μm channel to aid the phase selection. The cloud LWP is then estimated as 2/3 the product of optical depth and effective radius.

2.3. Comparison methods

Both case studies and comparisons are used in this paper to assess the uncertainties in τ, r_e, and LWP retrieved from CERES-MODIS for overcast stratus clouds over the Loess Plateau.

Due to the significant differences in temporal and spatial resolutions between the satellite and ground-based observations, the SACOL measurements must be scaled up to match the satellite observations. Cess et al. [7] demonstrated that the temporally averaged surface

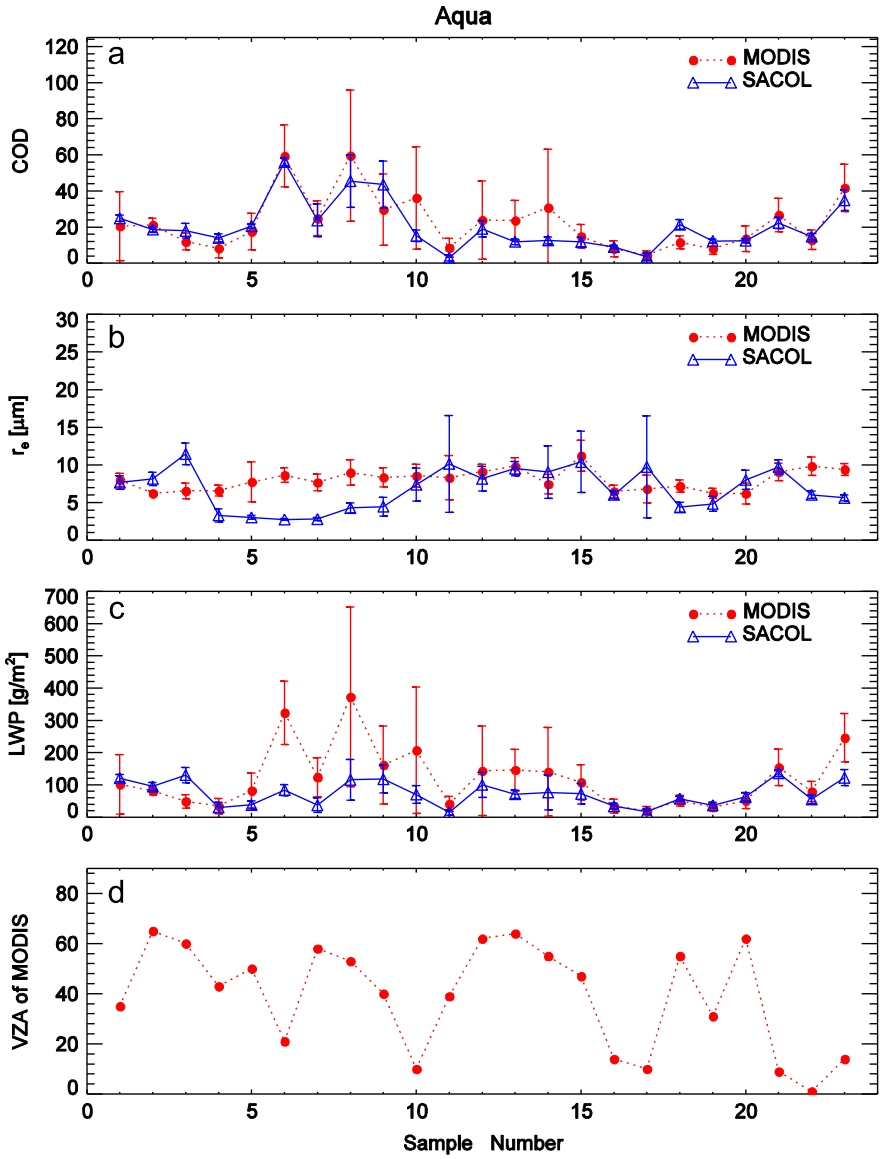

Fig. 2. Same as Fig. 1, but for Aqua.

observations should be equivalent to the spatially averaged satellite results in the statistical context. In this paper, the surface cloud properties averaged over a 1-h interval centered at the time of the satellite overpass are compared to the CERES-MODIS cloud properties averaged within a 20-km radius circle centered on the surface site. In order to minimize retrieval errors brought by the cloud 3D structure, the comparison cases are selected to correspond to the simplest situation, that is, the single layer, overcast conditions. Data recorded on days having rain/snow measurements and/or surface albedos larger than 0.3 were not used in this analysis. For case studies, other ground-based auxiliary observations are utilized to discuss possible sources of errors for those cases having large biases.

3. Result and discussion

3.1. Statistical analysis

The surface-retrieved daytime cloud microphysical properties are compared with the matched Terra and Aqua samples (shown in Figs. 1–3). The means, standard deviations of the differences, and linear correlation coefficients between the Terra/Aqua MODIS retrievals and surface results are summarized in Table 2. Figs. 1 and 2 show the time series (sample number is ordered from January 2008 to June 2010) of the respective Terra and Aqua cloud optical depths, cloud effective radii, and cloud liquid water paths along with their surface-derived counterparts for single layer, overcast stratus clouds at the SACOL. The error bars on the satellite and SACOL data points indicate the corresponding standard deviation. Since SACOL is located within a semi-arid, monsoon boundary zone, where significant low-level water vapor concentrations from the ocean occur infrequently, there are few overcast water cloud events: 27 for Terra and 23 for Aqua (Table 2). Fig. 3 shows the scatterplots of CERES-MODIS derived τ, LWP and r_e versus the matched surface retrievals using the samples in Figs. 1 and 2. The open circles and plus points, represent Terra and Aqua samples, respectively. The cloud optical depth (COD) scatter-plot (left panel) is generally lined up along the line of agreement, while the corresponding LWP (right panel) and r_e (middle panel) scatter plots show less correlation and overestimation, respectively.

The time series of CERES-MODIS cloud optical depth values (Figs. 1a and 2a), for the most part, closely track the variations of the surface retrievals and their correlation coefficients are 0.66 and 0.83, respectively, for Terra and Aqua. The averaged cloud optical depths from Terra are less than the surface retrievals by -4.7 with a standard error of 2.5, which is estimated by the standard deviation divided by the square root of the sample size. However, the averaged cloud optical depths from Aqua are greater than the surface retrievals by 2.1 with a standard error of 1.8 (Table 2). The COD is statistically underestimated for Terra and overestimated for Aqua. The relative discrepancy (-6.8) between the Terra and Aqua mean optical depths is likely due to differences in calibration of the 0.65-μm channels. Minnis et al. [34] reported that the Aqua VIS reflectance is 1–2% greater than that from Terra for the period through 2006. Since the Terra gain dropped by another 1% or so during 2009 (D. Doelling, 2011, personal communication), the cloud optical depths derived from Aqua data should be larger than those derived from Terra VIS data. The relative difference between the Terra and Aqua τ retrievals in this study is similar to that found by Dong et al. [13], that is, Terra COD is underestimated (-1.3) and Aqua COD is overestimated (2.5).

The r_e values derived from the Terra and Aqua MODIS mostly agree well with the corresponding surface-derived values for the last half of the period, but poorly in the first half of the period (Figs. 1b and 2b). The correlation is weak, but positive (Fig. 3). The results suggest that the satellite retrievals might lack some skill in measuring effective droplet radius in northwest of China. The Terra- and Aqua-retrieved r_e values overestimate their respective surface counterparts by 2.1 and 1.3 μm. However, if the large standard deviations of the differences (Table 2) are taken into account, the standard errors of the means are 0.62 and 0.60 μm, respectively, for Terra and Aqua. Thus, both the Terra and Aqua averages are likely overestimates, despite the given uncertainties in r_e derived from SACOL data. Different results were found over the SGP site, where Terra r_e is underestimated by -0.22 μm and Aqua r_e is overestimated by 0.34 μm [13].

Platnick [40] showed that the satellite retrieval of effective droplet size is typically biased high in optically thick stratus clouds because the reflected solar radiation emanates mostly from the larger droplets near the top of the cloud, while the surface-retrieved r_e, weighted by water mass in the cloud, represents the layer mean particle size. Due to the effective radius retrieved from the 3.7-μm reflectance more sensitivity to upper cloud microphysics relative to that from 1.6 μm and/or 2.1 μm which penetrate deeper, combining the effective radii from these different spectral bands can deduce whether or not the cloud particle size near the cloud top is larger or smaller than those below this altitude. And then some studies found that smaller droplets are located at the top of cloud [42,36–38,56]. Reasons for this phenomenon have been summarized in three aspects: warm rain process (e.g., [8–10]), cloud top entrainment [42] and 3-D radiative effects caused by cloud horizontal heterogeneity (e.g., [29,2,17,55]). Zhang and Platnick [56] showed that effective radius from the 3.7 μm, which is used in this study, is less sensitive to 3-D radiative effect but largely depend on cloud regime. Nakajima et al. [37] examined the sensitivity of cloud droplet radius to the vertical inhomogeneity of radius and found that effective radius from the 3.7 μm just conveys droplet size information in the optical depth range from 0 (cloud top) to 8 and is greatly influenced by smaller droplet at cloud top. In Figs. 1 and 2, most cases have COD larger than 8. The frequency of positive differences in r_e, i.e., r_e (CERES) $-$ r_e (surface), were about 76% for all those overcast cases. This might implies that the vertical variation of cloud droplet size in stratus cloud at SACOL generally follows the theory of typical adiabatic type of cloud but sometimes might be influenced by cloud top entrainment and/or drizzle.

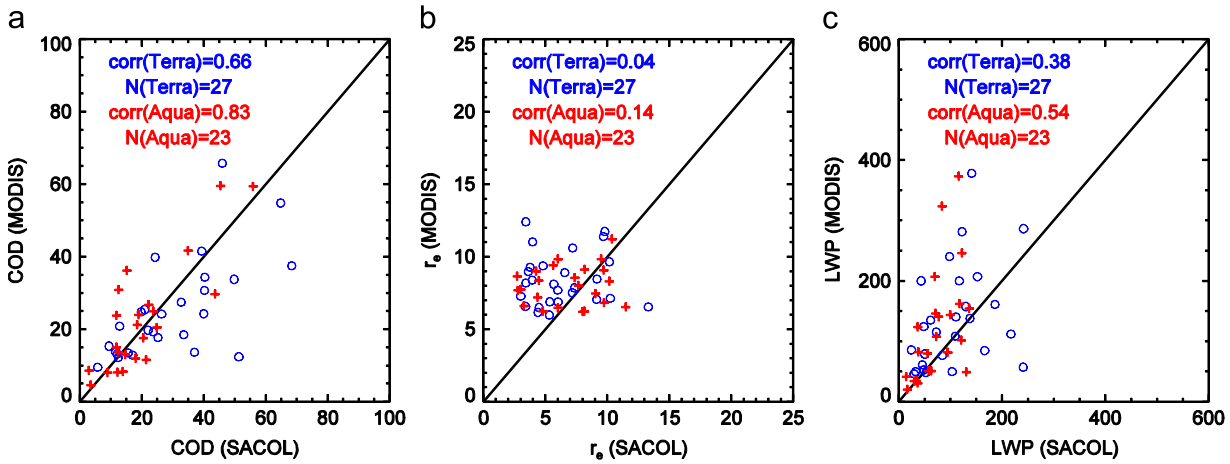

Fig. 3. Scatter plots of surface-derived (1-h average) and matched Terra MODIS-derived cloud microphysical properties (20-km radius average), (a) cloud liquid water path, (b) cloud optical depth, and (c) cloud effective radius, for daytime single layer, overcast stratus clouds over the SACOL.

Table 2
Mean and standard deviations (SD) of differences and linear correlation coefficients (Corr) of MODIS retrievals relative to surface results.

	No.	τ(CERES) − τ(sfc)			LWP(CERES) − LWP(sfc)			r_e(CERES) − r_e(sfc)		
		Mean	SD	Corr	Mean (g m^{-2})	SD	Corr	Mean (μm)	SD	Corr
Terra	27	−4.7	12.9	0.66	30.2	85.3	0.38	2.1	3.2	0.04
Aqua	23	2.1	8.4	0.83	47.4	79.6	0.54	1.3	2.9	0.14

The correlation coefficients between surface and satellite-derived LWP are 0.38 and 0.54, respectively, for Terra and Aqua. In Figs. 1c and 2c, the VISST cloud liquid water paths track the corresponding surface retrievals for most samples. Both the Terra and Aqua LWP means over SACOL overestimate the LWP retrieved from the brightness temperature of the ground-based microwave radiometer by an average of 30.2 and 47.4 g m^{-2} with standard deviations of 85.3 and 79.6 g m^{-2}, respectively (Table 2), values that are large considering that the corresponding mean LWP values are 105.8 and 73.6 g m^{-2}, respectively. The standard errors of the mean differences are 20.3 and 15.3 g m^{-2}, for Terra and Aqua, respectively. Thus, the mean differences are statistically significant. Because the VISST LWP is a product of τ and r_e, the errors in LWP are influenced by errors in both τ and r_e. When either r_e or τ is over or underestimated, the LWP will follow. Coincident over-estimates of τ and r_e for large values of cloud optical depth would cause extreme overestimates in LWP. While small cloud optical depths can be compensated by the large values of r_e, thus leading to good estimates of LWP. So the satellite-surface differences of LWP are not as large or statistically significant as for r_e. According to accuracy and validation report of CERES SSF cloud properties (url: ⟨http://eosweb.larc.nasa.gov/project/ceres/SSF/Quality_Summaries/CER_SSF_Aqua_Edition1B.html⟩, 2008), the Aqua LWP track the LWP from the ARM SGP microwave radiometer closely and is 10% larger than the ARM LWP. A later comparison performed over the ARM SGP [13] shows that the Aqua LWP exceeds its surface counterpart by 25.2%, while both the Terra average LWP is smaller than the surface mean by −2.4%. Herein, the Terra and Aqua LWP, on average, are respectively 71.8% and 28.5% larger than the SACOL LWP.

The satellite data can be used to provide an alternative estimate of LWP based on an assumption of adiabaticity [1]. Assuming that the satellite estimate of r_e corresponds to the top of the cloud, the density of water is 1 g cm^{-3}, and the liquid water content is distributed adiabatically through the depth of the cloud, the LWP can computed as LWP$=5/9\tau r_e$. Using this approach, the adiabatic LWP estimate is simply 0.83 times the definition used earlier. Using that conversion factor would yield mean differences of −9 and 0 g m^{-2} between the satellite and SACOL LWP values for Terra and Aqua, respectively. Painemal et al. [39] also found very good agreement between LWP determined from satellite-based microwave radiometer data and from satellite data analyzed with the CERES Edition 2 retrieval algorithm with the adiabatic assumption for marine stratocumulus clouds. Thus, the adiabatic approach may produce a more accurate value of mean LWP. However, use of the adiabatic value is probably more appropriate for optically thicker clouds for which r_e from the satellite is more representative of cloud top than the entire cloud. Determining when to use the adiabatic model is a subject for future research.

Generally speaking, there is a middling agreement between surface and CERES-MODIS cloud microphysical properties. The modest correlation coefficient and certain bias in τ and LWP indicate that the VISST can follow the variation of cloud parameters and provide relatively reliable values under single layer and overcast cloud condition at SACOL. However, the small correlation and significant bias of r_e is still a big puzzler. Dong et al. [13] compared

CERES-MODIS stratus cloud properties with ground-based measurements at the DOE ARM Southern Great Plains (SGP) site, showing analogous trends, high level of correlation in τ and LWP but modest correlation in r_e. But the Dong et al. [13] results produce much better agreement between the satellite-derived cloud properties at the ARM SGP than that at SACOL. Besides the skill of cloud retrieval algorithms, the biases in SACOL might be due to the other factors.

3.2. Case studies

To investigate uncertainty sources contributing to these differences between the satellite-derived and surface-retrieved cloud properties in Figs. 1 and 2, samples with large biases, such as Terra samples 12, and 24, and Aqua samples 13, were chosen for case studies. All possible contributions to the errors should be examined.

As mentioned in Section 2.3, the satellite-derived cloud properties averaged in a 20-km radius area centered on the SACOL corresponds, on average, to the surface retrievals averaged over 1-h interval centered at the time of each satellite overpass. For a typical low-level stratus cloud, the wind speed is about 10 m s^{-1}. Advection of the cloud during 1 h is nearly 36 km. This comparison method can deal with long-term dataset simply and usefully. However, wind speeds at cloud-height vary from case to case, indicating that the averaging area should vary with wind speed. It was found that a 0.5° radius area of GOES pixel-level cloud properties [12] or a 30-km × 30-km box [13] yielded essentially the same results as a more detailed analysis accounting for wind speed and direction over the ARM SGP. Thus, the average scheme used in this paper should be reasonable.

Cloud horizontal inhomogeneity can be inferred from the standard deviation (SD) of cloud optical depth in an average area or period. If the spatial variability of cloud optical properties within the averaging area is large, the surface instruments can be biased because they view only a small part of the deck seen by the satellite. Small clouds that partly cover satellite FOV (beam filling effect), and/or horizontally inhomogeneous clouds can also generated overestimation of effective particle radius [56]. It can be seen in Figs. 1 and 2 that data points with larger standard deviations mostly correspond to larger differences. Even if we select the single-layer and overcast cloud to reduce much of the three-dimensional structure influence on the retrieval algorithms and to mitigate the possible sampling differences between the retrievals from satellite and surface, the inhomogeneity at cloud top still cannot be avoided. This 3-D effect could also cause reflectance patterns to deviate from the plane-parallel model used in the satellite retrievals.

False identification of cloud phase can also makes a great contribution to the difference between satellite and surface retrievals. The phase determination is generally reliable for single-layered clouds. However, when thin cirrus clouds overlay a thick low-level cloud, phase detection becomes ambiguous because the spectral radiances are influenced by both cloud layers. Ice clouds generally decrease the amount of reflected solar infrared radiation relative to that for a liquid cloud. This effect can result in either too large value for water droplets or too small value for ice crystals depending on the final phase classification [24]. Additionally, the ability to discriminate ice and water particles at cloud top is much reduced when clouds may contain primarily super-cooled water droplets or perhaps a mixture of both ice and water (i.e., mixed phase).

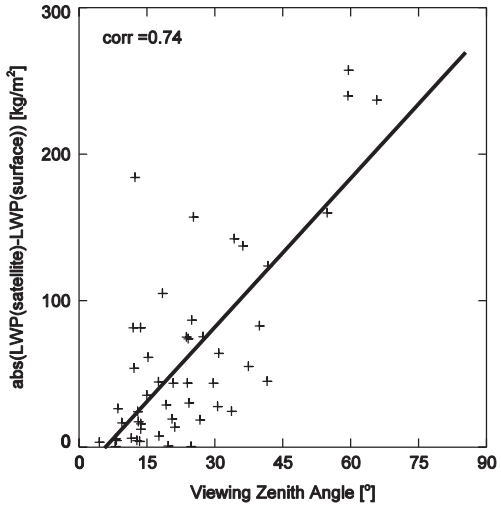

Fig. 4. The relationship between absolute value of biases in LWP and viewing zenith angle.

Besides cloud horizontal inhomogeneity and false identification of cloud phase, sun/satellite viewing geometry also influences the observed reflected and emitted radiance, and then results in retrieval errors in cloud optical properties. Loeb et al. [26] found that shadows from any cloud structure would tend to reduce the inferred optical depth when viewed in the forward direction at a high VZA, while the optical depth is enhanced in the cross-scattering view because of more side scatter by the cloud facets. And those types of differences become more pronounced with larger SZAs. Horváth and Davies [19] found a slight increase in LWP with VZA, ~20% at VZA between 60° and 70°. In this study, the absolute value of CERES-MODIS LWP bias increase with VZA is also identical (Fig. 4). Heck et al. [18] averaged the CERES-MODIS data over non-polar land for one month and found that neither τ nor r_e increased significantly with VZA between 0° and 70° implying that LWP did not vary much either. However, they found that average cloud fraction increased from around 40% to 50% for the same range of VZA. Thus, some areas classified as overcast at high VZAs could, in fact, consist of broken clouds, which would affect the assumptions used here.

For Terra sample 12 (Fig. 5), taken at 0305 UTC, 21 July 2009, the satellite derived τ, LWP and r_e are overestimated by 19.9, 236.9 g m^{-2} and 4.5 μm respectively relative to the SACOL retrievals. Both standard RGB and pseudo-color MODIS images are shown in Fig. 5 with the sky condition captured by the TSI. The pseudo-color MODIS imagery, providing the larger-scale context for interested area of case study, is created by using the 2.1 μm, 0.86 μm, and 0.66 μm radiances to determine the intensities of red,

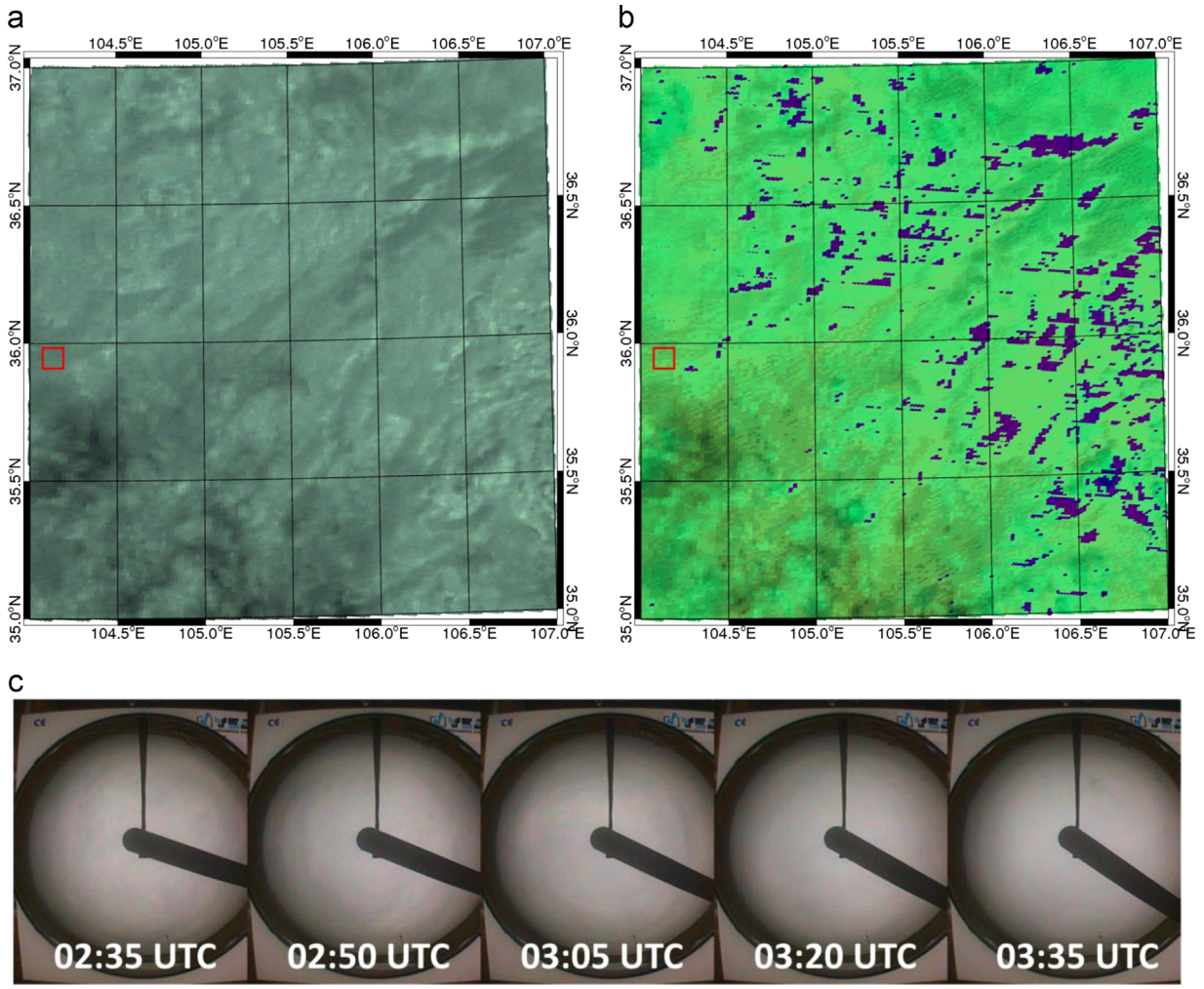

Fig. 5. (a) MODIS true color RGBs images, (b) MODIS false color RGBs composite images, which uses 2.1, 0.86, and 0.66 μm as the red, green, and blue channels, over SACOL (red box) and (c) sky condition from Total Sky Image (TSI) for Terra sample 12 (0305UTC, 21 July 2009). Typically, high clouds appear blue or bluish-purple and low clouds white, and the surface near-black. (For interpretation of the references to color in this figure legend, the reader is referred to the web version of this article.)

green and blue, respectively. This kind of imagery is convenient for showing most of the information that normally requires two to three images to convey owing to the differences of cloud radiance properties in these three channels. Typically, high clouds appear blue and low clouds white. Clear areas are primarily green and brown. According to the MODIS images, thick water clouds, which might overlaid by some ice cloud, are over the site during the satellite overpass. Because the all single-layer cases are selected through a batch processing, which just guarantee the single layer condition in the 20-km radius average circle, the ice cloud outside of this area still has the potential to contaminate this case. The TSI photos also demonstrate that there is 100% cloudiness before and after the satellite overpass. The clouds appear to be quite thick. For this case, satellite retrieved cloud effective radius is easily overestimated because satellite spectral band cannot penetrate deep in cloud. Overestimates of τ and r_e for large cloud optical depth should certainly lead to extreme overestimates in LWP. Meanwhile, the satellite VZA is very large (64°), and the number of valid MODIS pixels in the 20 km-radius circle around the SACOL is only 31. All these factors could be major contributors to the large bias in this sample.

Terra sample 24 (0305 UTC, 05 May 2010) is given in Fig. 6. The satellite-derived τ and LWP are -39.0 and -184.1 g m^{-2}, respectively, less than their SACOL counterparts. And r_e from the CERES MODIS retrieval is slightly greater (0.4 μm) than the SACOL retrieval. Fig. 6c shows the backscatter intensity vertical profiles over the SACOL site after corrections for range, overlap and Rayleigh scattering [20]. The backscattered intensities from clouds are generally stronger than those from aerosols. The white dotted lines in the MPL profiles indicate the averaging period for the surface observations, i.e., the 1-h interval centered at the time of satellite overpass. As Fig. 6a and b shows, liquid cloud layers over the SACOL site are low and continuous, while some of the cirrus clouds are north of

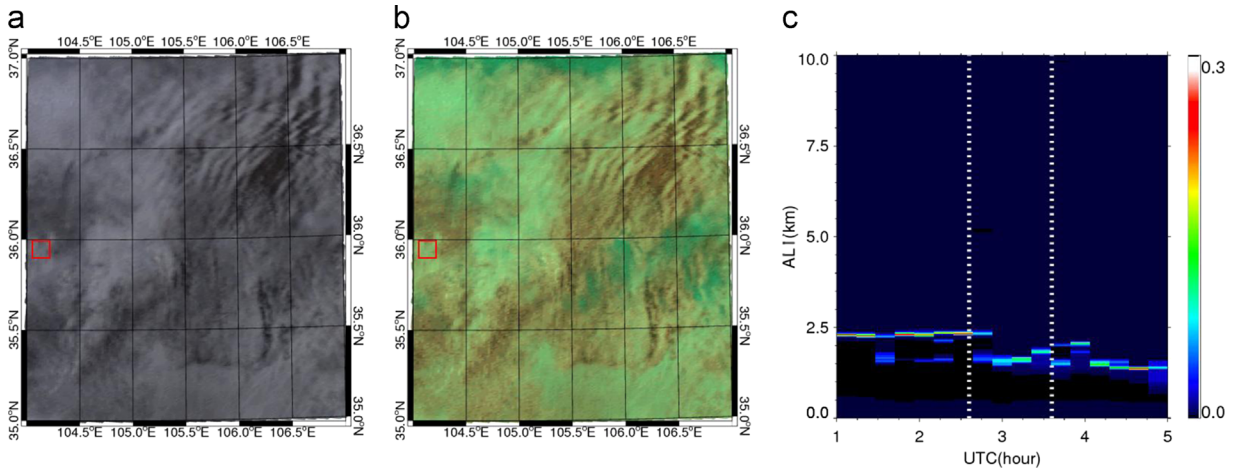

Fig. 6. (a, b) MODIS 3-channel composite images over SACOL (red box) and (c) Micro-Pulse Lidar (MPL) normalized relative backscatter for Terra sample 24 (0305UTC, 5 May 2010), white dotted lines indicate the 1-h interval centered at the time of satellite overpass. (For interpretation of the references to color in this figure legend, the reader is referred to the web version of this article.)

the site. Close examination of the MPL normalized relative backscatter in Fig. 6c reveals that clouds over the site are not always single layered; the cloud heights varied from 1500 to 2400 m in the average period. Obviously, cloud horizontal inhomogeneity makes a great contribution to a large bias in τ but small influence on r_e. It is not surprising that 3.7-μm r_e is not very sensitivity to cloud inhomogeneity [56]. Additionally, the VZA for this sample is large (64°), which might be another important reason for such large bias between satellite and surface retrievals.

Fig. 7 shows the MODIS images, and sky condition from TSI for Aqua sample 13, taken at 0705 UTC, 8 September 2009. The τ, LWP, and r_e differences between the satellite and surface measurements are 4.9, 43.7 g m^{-2}, and 0.9 μm, respectively. The satellite imagery for this sample suggests that a layer of liquid cloud was flowing over the SACOL site (Fig. 7a and b). Meanwhile, close inspection of the sky cover recorded by the TSI during the period of surface averaging illustrates that overcast stratus clouds always covered the SACOL while the thickness of cloud was inhomogeneous (Fig. 7c). Some parts of the cloud are opaque; but others are semi-transparent. This kind of inhomogeneity might contribute to the bias. Moreover, the VZA for this sample reaches 62°, resulting in only 37 valid pixels for this sample. Both the horizontal inhomogeneity and large VZA likely lead to the overestimation of the satellite-retrievals.

Other selected samples, which are without the simultaneous observation of MPL and/or TSI, are discussed briefly below. For some Terra (3, 6, 7, 8, 12, 13 and 26) and Aqua (1, 5, 15, 19 and 22) samples, cirrus clouds might be flowing over low cloud deck and/or mix-phase clouds occur over the SACOL site according to the MODIS cloud images. Cirrus contamination likely contributed to the divergence in those samples. The statistics on cases without cirrus contaminated is summarized in Table 3. The LWP and r_e from Terra show better agreement with surface matched retrievals. Owing to limited samples, retrievals from Aqua do not show much improvement. Although raining condition has been excluded at the beginning, drizzle occurring in cloud might be a potential contributor to large biases for those cases. But due to the limitation of instruments at SACOL, the drizzle information cannot be derived. So it is hard to validate the drizzle influences on these cases. It is also worth noting that satellite derived cloud properties for those cases (Terra sample 5–10, Aqua sample to 4–8) in Spring do not show a good agreement with surface retrievals. Over Loess Plateau, Spring is the season of dust storm and companies with high aerosol number concentration. For limited liquid water source, large aerosol concentration means more cloud condensation nuclei, smaller cloud droplet and brighter cloud. Satellite retrieved cloud droplet size might be overestimated. In additional, due to large viewing angles, some samples with few valid pixels in averaging area can also lead to a large bias, such as Terra sample 2, 3, 12, 13, 17, 24, 25 and Aqua sample 2, 3, 12, 13, 20.

4. Conclusion

Cloud plays a very important role in climate system and hydrological cycle, especially over those semi-arid regions. However, understanding cloud effects on climate resulting from cloud feedbacks is still extremely challenging. The first step for solving this problem is to understand the accuracies and stabilities of those global climate datasets. Herein, cloud properties derived from CERES-MODIS cloud retrieval algorithms have been compared with well-validated surface observations at SACOL from January 2008 to June 2010 under overcast and single-layer condition during daytime. From a statistical analysis, both Terra and Aqua derived cloud optical depth and LWP could generally track the variation of the surface counterparts with high and modest correlation, respectively. While cloud effective radius values generally did not follow the surface retrieval variations and are only weakly correlated, the means were very close. The mean differences between the Terra and surface retrievals are -4.7 ± 12.9, 2.1 ± 3.2 μm and 30.2 ± 85.3 g m^{-2} for τ, r_e and LWP, respectively. And the corresponding differences for Aqua are

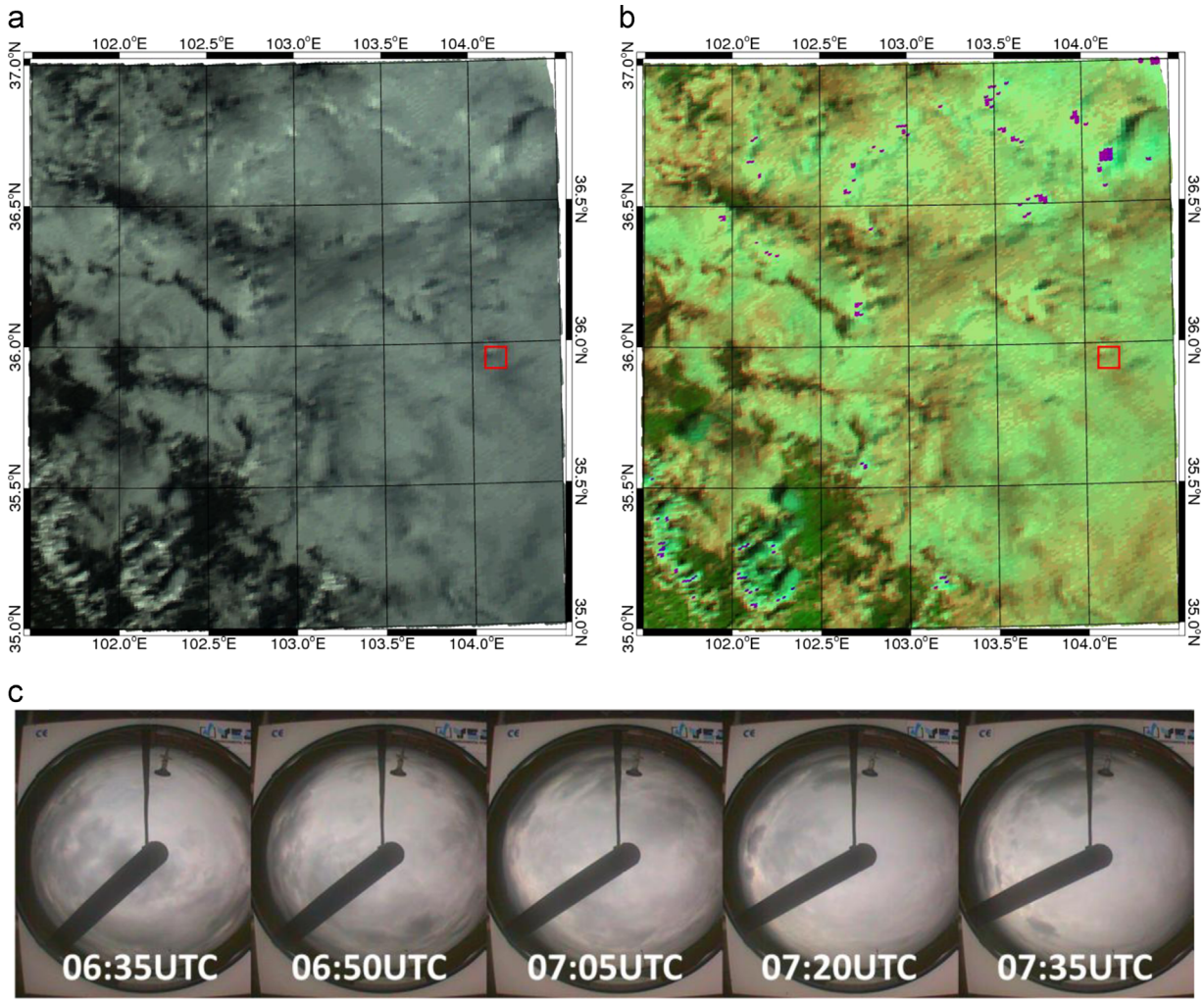

Fig. 7. Same as Figs. 5 and 6, but for Aqua sample 13 (0705UTC, 8 September 2009).

Table 3
Same as Table 2, but only for cloud without cirrus contamination based on MODIS cloud images.

	No.	τ(CERES) − τ(sfc)			LWP(CERES) − LWP(sfc)			r_e(CERES) − r_e(sfc)		
		Mean	SD	Corr	Mean (g m^{-2})	SD	Corr	Mean (μm)	SD	Corr
Terra	20	−7.4	12.6	0.66	4.1	67.3	0.53	1.7	2.4	0.37
Aqua	18	3.3	9.1	0.83	56.2	87.5	0.54	0.9	3.1	0.05

2.1 ± 8.4, 1.2 ± 2.9 μm and 47.4 ± 79.6 g m^{-2}, respectively. Comparing with previous studies in other areas, biases in τ (CERES-SACOL) over the Loess Plateau share the same signs but have larger values. Small discrepancies between Aqua and Terra biases in cloud microphysical properties can be explained by uncorrected calibration difference. The sources for the large variations in the differences between the surface and satellite-retrieved r_e are many. The differences between satellite and surface derived cloud liquid water path seem to increase with increasing VZA, most likely as a result of the reduced number of valid pixels and, perhaps, some parallax error. Larger SZAs can enhance the differences. It has been found that cloud inhomogeneity, phase differences, drizzle, and large angles may be major contributors to the differences between the satellite and surface retrievals through case studies. Additionally, large uncertainties in LWP and r_e values from the surface retrievals for optically thin clouds also contribute to the differences.

Comparing the similar validation operated in other sites, the CERES-MODIS cloud properties over the interior of China still need to be improved. The Terra optical depth retrievals are underestimated, most likely due to the calibration bias noted by Minnis et al. [34]. Normalizing the Terra calibrations to Aqua, as planned for future editions of the CERES data [35], should mitigate the Terra

optical depth bias. The number of selected samples in this study is not adequate due to limited occurrences of overcast stratus at SACOL, then additional analysis and complete validations for cirrus, mix-phase cloud, and so on, are still needed herein. It is also necessary to conduct validation by comparing with both surface observation and other passive and active sensors on satellites, such as CloudSat, CALIPSO, in this area. Exhaustive validation of the datasets from space will promote the advance of satellite retrieval algorithm and improve the understanding of mechanism of climate changes.

Acknowledgments

SACOL was sponsored by the Lanzhou University through the 985 Program. This study is supported by the National Basic Research Program of China (2013CB955802 and 2012CB955301), National Natural Science Foundation of China (41375031), the Program for Changjiang Scholars and Innovative Research Team in University (IRT1018), and China 111 Project (No. B13045). Support for Yuhong Yi and Sunny Sun-Mack was provided by the NASA CERES Project. Thanks to Tian Zhou, Beidou Zhang and Jianrong Bi for their efforts in providing ground-based observations.

References

[1] Bennartz R. Global assessment of marine boundary layer cloud droplet number concentration from satellite. J Geophys Res 2007;112:D02201. http://dx.doi.org/10.1029/2006JD007547.
[2] Boeke RC. Biases in droplet radii and optical depths of marine stratocumulus retrieved from MODIS imagery.(M.S. thesis). Corvallis: Oregon State University; 2009.
[3] Bony S, Colman R, Kattsov VM, Allan RP, Bretherton CS, Dufresne J, et al. How well do we understand and evaluate climate change feedback processes? J Clim 2006;19:3445–82.
[4] Cess RD, Potter GL, Blanchet JP, Boer GJ, Ghan SJ, Kiehl JT, et al. Interpretation of cloud-climate feedback as produced by 14 atmospheric general circulation models. Science 1989;245:513–6.
[5] Cess RD, Potter GL, Blanchet JP, Boer GJ, Del Genio AD, Déqué M, et al. Intercomparison and interpretation of climate feedback processes in 19 atmospheric general circulation models. J Geophys Res 1990;95(D10):16601–15.
[6] Cess RD, Zhang MH, Ingram WJ, Potter GL, Alekseev V, Barker HW, et al. Cloud feedback in atmospheric general circulation models: an update. J Geophys Res 1996;101(D8):12791–4. http://dx.doi.org/10.1029/96JD00822.
[7] Cess RD, Zhang MH, Zhou Y, Jing X, Dvortsov V. Absorption of solar radiation by clouds: interpretations of satellite, surface, and aircraft measurements. J Geophys Res 1996;101:23299–309.
[8] Chang FL, Li Z. Estimating the vertical variation of cloud droplet effective radius using multispectral near-infrared satellite measurements. J Geophys Res 2002;107(D15):4257. http://dx.doi.org/10.1029/2001JD000766.
[9] Chang FL, Li Z. Retrieving vertical profiles of water-cloud droplet effective radius: algorithm modification and preliminary application. J Geophys Res 2003;108(D24):4763. http://dx.doi.org/10.1029/2003JD003906.
[10] Chen R, Wood R, Li Z, Ferraro R, Chang F-L. Studying the vertical variation of cloud droplet effective radius using ship and space-borne remote sensing data. J Geophys Res 2008;113:D00A02. http://dx.doi.org/10.1029/2007JD009596.
[11] Dong X, Mace GG, Minnis P, Young DF. Arctic stratus cloud properties and their impact on the surface radiation budget: selected cases from FIRE ACE. J Geophys Res 2001;106:15297–312.
[12] Dong X, Minnis P, Mace GG, Smith Jr. WL, Poellot M, Marchand R, et al. Comparison of stratus cloud properties deduced from surface, GOES, and aircraft data during the March 2000 ARM Cloud IOP. J Atmos Sci 2002;59:3265–84.
[13] Dong X, Minnis P, Xi B, Sun-Mack S, Chen Y. Comparison of CERES-MODIS stratus cloud properties with ground-based measurements at the DOE ARM Southern Great Plains site. J Geophys Res 2008;113:D03204. http://dx.doi.org/10.1029/2007JD008438.
[14] Dufresne J-L, Bony S. An assessment of the primary sources of spread of global warming estimates from coupled atmosphere-climate models. J Clim 2008;21:5135–44. http://dx.doi.org/10.1175/2008JCLI2239.1.
[15] Fu Q, Johanson CM, Wallace JM, Reichler T. Enhanced mid-latitude tropospheric warming in satellite measurements. Science 2006;312:1179.
[16] Hansen J, Lacis A, Rind D, Russell P, Stone P, Fung I, et al. Climate sensitivity: analysis of feedback mechanisms. In: Hansen JE, Takahashi T, editors. Climate processes and climate sensitivity. Geophysical monograph, vol. 29. Washington, DC: American Geophysical Union; 1984. p. 130–63.
[17] Hayes CR, Coakley Jr. JA, Tahnk WR. Relationships among properties of marine stratocumulus derived from collocated CALIPSO and MODIS observations. J Geophys Res 2010;115:D00H17. http://dx.doi.org/10.1029/2009JD012046.
[18] Heck PW, Minnis P, Young DF, Sun-Mack S. Angular variations of cloud properties from VIRS and MODIS data. In: Proceedings of 11th AMS conference on atmospheric radiation, Ogden, UT; 2002. p. 148–51.
[19] Horváth Á, Davies R. Comparison of microwave and optical cloud water path estimates from TMI, MODIS, and MISR. J Geophys Res 2007;112:D01202. http://dx.doi.org/10.1029/2006JD007101.
[20] Huang J, Huang Z, Bi J, Zhang W, Zhang L. Micro-pulse Lidar measurements of aerosol vertical structure over the Loess Plateau. Atmos Ocean Sci Lett 2008;1:8–11.
[21] Huang J, Zhang W, Zuo J, Bi J, Shi J, Wang X, et al. An overview of the semi-arid climate and environment research observatory over the Loess Plateau. Adv Atmos Sci 2008;25:1–16.
[22] Huang J, He M, Yan H, Zhang B, Bi J, Jin Q. A study of liquid water path and precipitable water vapor in Lanzhou area using ground-based microwave radiometer. Chin J Atmos Sci 2010;34:548–58.
[23] Joseph E, Min Q. Assessment of multiple scattering and horizontal inhomogeneity in IR radiative transfer calculations of observed thin cirrus clouds. J Geophys Res 2003;108(D13):4380. http://dx.doi.org/10.1029/2002JD002831.
[24] Kawamoto K, Minnis P, Smith Jr. WL. Cloud overlapping detection algorithm using solar and IR wavelengths with GOES data over the ARM/SGP site. In: Proceedings of 11th ARM science team meeting, Atlanta, GA, DOE; 2001.
[25] Liljegren JC, Clothiaux EE, Mace GG, Kato S, Dong X. A new retrieval for cloud liquid water path using a ground-based microwave radiometer and measurements of cloud temperature. J Geophys Res 2001;106:14485–500.
[26] Loeb NG, Varnai T, Winker DM. Influence of sub-pixel scale cloud-top structure on reflectances from overcast stratiform cloud layers. J Atmos Sci 1998;55:2960–73.
[27] Mace GG, Zhang Y, Platnick S, King MD, Minnis P, Yang P. Evaluation of cirrus cloud properties derived from MODIS data using cloud properties derived from ground-based observations collected at the ARM SGP site. J Appl Meteorol 2005;44:221–40. http://dx.doi.org/10.1175/JAM2193.1.
[28] Manabe S, Wetherald RT. The effects of doubling the CO_2 concentration on the climate of a general circulation model. J Atmos Sci 1975;32:3–15.
[29] Marshak A, Platnick S, Várnai T, Wen G, Cahalan RF. Impact of three-dimensional radiative effects on satellite retrievals of cloud droplet sizes. J Geophys Res 2006;111:D09207. http://dx.doi.org/10.1029/2005JD006686.
[30] Min Q, Harrison LC. Cloud properties derived from surface MFRSR measurements and comparison with GOES results at the ARM SGP site. J Geophys Lett 1996;23(13):1641–4. http://dx.doi.org/10.1029/96GL01488.
[31] Min Q, Joseph E, Duan M. Retrievals of thin cloud optical depth from a multifilter rotating shadowband radiometer. J Geophys Res 2004;109:D02201. http://dx.doi.org/10.1029/2003JD003964.
[32] Min Q, Minnis P, Khaiyer M. Comparison of cirrus optical depths derived from GOES 8 and surface measurements. J Geophys Res 2004;109:D15207. http://dx.doi.org/10.1029/2003JD004390.
[33] Minnis P, Trepte QZ, Sun-Mack S, Chen Y, Doelling DR, Young DF, et al. Cloud detection in non-polar regions for CERES using TRMM VIRS and Terra and Aqua MODIS data. IEEE Trans Geosci Remote Sens 2008;46:3857–84.
[34] Minnis P, Doelling DR, Nguyen L, Miller WF, Chakrapani V. Assessment of the visible channel calibrations of the TRMM VIRS and MODIS on Aqua and Terra. J Atmos Ocean Technol 2008;25:385–400.

[35] Minnis P, Sun-Mack S, Young DF, Heck PW, Garber DP, Chen Y, et al. CERES Edition-2 cloud property retrievals using TRMM VIRS and Terra and Aqua MODIS data, Part I: algorithms. IEEE Trans Geosci Remote Sens 2011;49:4374–400.
[36] Minnis P, Sun-Mack S, Chen Y, Khaiyer MM, Yi Y, Ayers JK, et al. CERES Edition-2 cloud property retrievals using TRMM VIRS and Terra and Aqua MODIS data, Part II: examples of average results and comparisons with other data. IEEE Trans Geosci Remote Sens 2011;49:4401–30.
[37] Nakajima TY, Suzuki K, Stephens GL. Droplet growth in warm water clouds observed by the A-Train. Part I: sensitivity analysis of the MODIS-derived cloud droplet size. J Atmos Sci 2010;67:1884–96.
[38] Nakajima TY, Suzuki K, Stephens GL. Droplet growth in warm water clouds observed by the A-Train. Part II: a multi-sensor view. J Atmos Sci 2010;67:1897–907.
[39] Painemal D, Minnis P, Ayers JK, O'Neill L. GOES-10 microphysical retrievals in marine warm clouds: multi-instrument validation and daytime cycle over the Southeast Pacific. J Geophys Res 2012;117:D19212. http://dx.doi.org/10.1029/2012JD017822.
[40] Platnick S. Vertical photon transport in cloud remote sensing problems. J Geophys Res 2000;105:22919–35.
[41] Randall DA, Wood RA, Bony S, Colman R, Fichefet T, Fyfe J, et al. Climate models and their evaluation. In: Solomon S, Qin D, Manning M, Chen Z, Marquis M, Averyt KB, Tignor M, Miller HL, editors. Climate change 2007: the physical science basis. contribution of working group I to the fourth assessment report of the intergovernmental panel on climate change. Cambridge (United Kingdom), New York (NY, USA): Cambridge University Press; 2007.
[42] Seethala C, Horváth Á. Global assessment of AMSR-E and MODIS cloud liquid water path retrievals in warm oceanic clouds. J Geophys Res 2010;115:D13202. http://dx.doi.org/10.1029/2009JD012662.
[43] Soden BJ, Held IM. An assessment of mate feedbacks in coupled ocean–atmosphere models. J Clim 2006;19:3354–60.
[44] Spangenberg DA, Heck P, Minnis P, Trepte Q, Sun-Mack S, Uttal T., et al. Artic cloud properties derived from multispectral MODIS and AVHRR data. In: Proceedings of 11th AMS conference of cloud physics, Ogden, Utah; 2002.
[45] Stephens GL. Cloud feedbacks in the climate system: a critical review. J Clim 2005;18:237–73.
[46] Uttal T, Sun-Mack S, Minnis P, Key J. Comparison of surface and satellite measurements of Arctic cloud properties. In: Proceedings of the seventh conference on polar meteorology and oceanography and joint symposium on high-latitude climate variations, Hyannis, MA; 2003.
[47] Trepte Q, Minnis P, Arduini RF. Daytime and nighttime polar cloud and snow identification using MODIS data. Proc SPIE Int Soc Opt Eng 2002;4891:449–59.
[48] Waliser D, Li F, Woods C, Austin R, Bacmeister J, Chern J, et al. Cloud ice: a climate model challenge with signs and expectations of progress. J Geophys Res 2009;114:D00A21. http://dx.doi.org/10.1029/2008JD010015.
[49] Wang T, Min Q. Retrieving optical depths of optically thin and mixed-phase clouds from MFRSR measurements. J Geophys Res 2008;113:D19203. http://dx.doi.org/10.1029/2008JD009958.
[50] Wang G, Huang J, Guo W, Zuo J, Wang J, Bi J, et al. Observation analysis of land-atmosphere interactions over the Loess Plateau of northwest China. J Geophys Res 2010;115:D00K17. http://dx.doi.org/10.1029/2009JD013372.
[51] Webb MJ, Senior CA, Sexton DMH, Ingram WJ, Williams KD, Ringer MA, et al. On the contribution of local feedback mechanisms to the range of climate ensitivity in two GCM ensembles. Clim Dyn 2006;27:17–38. http://dx.doi.org/10.1007/s00382-006-0111-2.
[52] Wielicki BA, Cess RD, King MD, Randall DA, Harrison EF. Mission to planet Earth: role of clouds and radiation in climate. Bull Am Meteorol Soc 1995;76:2125–53.
[53] Wielicki BA, Barkstrom BR, Harrison EF, Lee III RB, Smith GL, Cooper JE. Cloud and the Earth's radiant energy system (CERES): an Earth observing system experiment. Bull Am Meteorol Soc 1996;77:853–68.
[54] Wielicki BA, Barkstrom BR, Baum BA, Charlock TP, Green RN, Kratz DP, et al. Clouds and the Earth's Radiant Energy System (CERES): algorithm overview. IEEE Trans Geosci Remote Sens 1998;36:1127–41.
[55] Wolters ELA, Deneke HM, van den Hurk BJJM, Meirink JF, Roebeling RA. Broken and inhomogeneous cloud impact on satellite cloud particle effective radius and cloud-phase retrievals. J Geophys Res 2010;115:D10214. http://dx.doi.org/10.1029/2009JD012205.
[56] Zhang ZB, Platnick S. An assessment of differences between cloud effective particle radius retrievals for marine water clouds from three MODIS spectral bands. J Geophys Res 2011;116:D20215. http://dx.doi.org/10.1029/2011jd016216.
[57] Zheng X, Albrecht B, Jonson H, Khelif D, Feingold G, Minnis P, et al. Observations of the boundary layer, cloud, and aerosol variability in the southeast Pacific coastal marine stratocumulus during VOCALS-Rex. Atmos Chem Phys 2011;11:9943–59.